Metal content of multicrystalline silicon for solar cells and its impact on minority carrier diffusion length

A. A. Istratov[a] and T. Buonassisi
University of California and Lawrence Berkeley National Laboratory, MS 62R0203, 1 Cyclotron Road, Berkeley, California 94720

R. J. McDonald and A. R. Smith
Lawrence Berkeley National Laboratory, MS 72R0150, 1 Cyclotron Road, Berkeley, California 94720

R. Schindler
Fraunhofer Institute for Solar Energy Systems, Heidenhofstrasse 2, D-79110 Freiburg, Germany

J. A. Rand
Astropower, Solar Park, Newark, Delaware 19716-2000

J. P. Kalejs
RWE Schott Solar, Incorporated, 4 Suburban Park Drive, Billerica, Massachusetts 01821-3980

E. R. Weber
University of California, Department of Materials Science and Engineering, 374 Hearst Mining Building, Berkeley, California 94720

(Received 29 May 2003; accepted 25 August 2003)

Instrumental neutron activation analysis was performed to determine the transition metal content in three types of silicon material for cost-efficient solar cells: Astropower silicon-film sheet material, Baysix cast material, and edge-defined film-fed growth (EFG) multicrystalline silicon ribbon. The dominant metal impurities were found to be Fe (6×10^{14} cm^{-3} to 1.5×10^{16} cm^{-3}, depending on the material), Ni (up to 1.8×10^{15} cm^{-3}), Co (1.7×10^{12} cm^{-3} to 9.7×10^{13} cm^{-3}), Mo (6.4×10^{12} cm^{-3} to 4.6×10^{13} cm^{-3}), and Cr (1.7×10^{12} cm^{-3} to 1.8×10^{15} cm^{-3}). Copper was also detected (less than 2.4×10^{14} cm^{-3}), but its concentration could not be accurately determined because of a very short decay time of the corresponding radioactive isotope. In all samples, the metal contamination level would be sufficient to degrade the minority carrier diffusion length to less than a micron, if all metals were in an interstitial or substitutional state. This is a much lower value than the actual measured diffusion length of these samples. Therefore, most likely, the metals either formed clusters or precipitates with relatively low recombination activity or are very inhomogeneously distributed within the samples. No significant difference was observed between the metal content of the high and low lifetime areas of each material. X-ray microprobe fluorescence spectrometry mapping of Astropower mc-Si samples confirmed that transition metals formed agglomerates both at grain boundaries and within the grains. It is concluded that the impact of metals on solar cell efficiency is determined not only by the total metal concentration, but also by the distribution of metals within the grains and the chemical composition of the clusters formed by the metals. © *2003 American Institute of Physics.*
[DOI: 10.1063/1.1618912]

I. INTRODUCTION

In order to reduce the cost of installed solar panels and make solar energy competitive with conventional sources of electricity, several low-cost ribbon-growth, sheet, and cast technologies were developed for the high-volume production of multicrystalline silicon (mc-Si). However, the relatively low per-wafer cost of these materials is offset with a lower light-to-electricity conversion efficiency of the mc-Si cells as compared to single-crystalline silicon solar cells. For example, the highest efficiency reported to-date for single-crystalline solar cell is 24.7%, whereas the best efficiency reported for multicrystalline solar cell is currently 19.8%.[1] The efficiencies of production-grade cells are typically 6%–9% lower than those values. The origin of the relatively low efficiency of mc-Si cells as compared to single-crystalline cells has been debated for many years, but there is still no definite answer as to what defects are primary culprits. The problem is exacerbated by a wide variety of defects inhomogeneously distributed within the mc-Si material, such as dislocations, grain boundaries, oxygen clusters, microscopic intragranular defects, and metal impurities. Hence, it is very difficult to determine the recombination properties of individual defects and identify the most detrimental ones.

Transition metal contamination is thought to be one of the major factors contributing to the lifetime degradation. Metals can be introduced into mc-Si wafers from the feed-

[a]Author to whom correspondence should be addressed; electronic mail: istratov@socrates.berkeley.edu

stock during the ribbon/sheet growth and can be added during the subsequent production steps. It is known from practical experience that lower grade silicon feedstock partly accounts for the difference in efficiency between high-volume production cells and research and development cells. While gettering can reduce the amount of metal contaminants in the cells, additional contaminants can also be introduced during processing due to the relatively lenient requirements for the cleanliness of the production environment at a typical photovoltaic facility.

The transition metals and their precipitates are known to be highly recombination active in silicon (see, e.g., Refs. 2–5), and may be one of the culprits of the efficiency degradation of solar cells. Unfortunately, the published data on metal content of multicrystalline silicon are scarce. The only recent study of photovoltaic-grade mc-Si is that of Macdonald *et al.*,[6] who performed neutron activation analysis (NAA) of cast mc-Si before and after phosphorus diffusion gettering. Before gettering, they found 10^{14} cm^{-3} of Fe, 2×10^{13} cm^{-3} of Cu, 2×10^{13} cm^{-3} of Cr, 4×10^{11} cm^{-3} of Co, 1.5×10^{11} cm^{-3} of Ag, 2×10^{13} cm^{-3} of Zn, and 7×10^{12} cm^{-3} of Sn, along with some As and Sb. Phosphorus diffusion gettering reduced the metal contamination levels by 60%–90% (e.g., iron concentration was reduced to approximately 2.3×10^{13} cm^{-3}), but was not capable of removing the metals completely.[6] There are no data on how materials grown with different technologies, or samples of the same type of material with different minority carrier diffusion lengths, compare in terms of their metal content. Thus, a comparative study of transition metal contamination levels of several types of mc-Si materials could provide valuable information on the role of transition metals in reduction of minority carrier diffusion length.

Another important problem of silicon photovoltaics is to understand the origin of the differences between grains with high and low minority carrier diffusion length, commonly observed in all mc-Si materials. In addition to low charge collection efficiency, areas with low diffusion length may also have lower than average local open-circuit voltage, thus shunting the good areas of the cell and disproportionally reducing the overall cell efficiency.[7,8] The studies of iron precipitation kinetics in ''bad grains'' (grains with low diffusion length) and in ''good grains'' (grains with high diffusion length) revealed that bad grains had much higher density of precipitation sites for metals.[9] The nature of these precipitation sites is not certain despite recent efforts to find them by transmission electron microscopy.[10] It was suggested that transition metals decorate intragranular microdefects (the generic term used to describe these microscopic defects of uncertain origin), thus increasing their recombination activity.[9] Experiments with intentional contamination of Czochralski (CZ), float-zone (FZ), and mc-Si materials with iron, and the subsequent gettering of the contaminated samples, demonstrated that the minority carrier diffusion length dropped significantly after intentional iron contamination in all three types of samples and then increased to almost its initial value after aluminum gettering in CZ and FZ silicon, but was hardly improved by gettering in mc-Si and remained at a very low value.[11] This led to the hypothesis that transition metals may form gettering-resistant complexes within mc-Si wafers.[12] This conclusion was supported by the synchrotron radiation-based microprobe x-ray fluorescence (μ-XRF) and x-ray absorption studies of McHugo *et al.*[13–15] These findings indicate that metal impurities may be responsible for the poor performance of bad grains. However, it was not clear until now whether the total metal concentration was higher in the ''bad'' areas than in the ''good'' areas, or if the difference was primarily in the chemical state and distribution of transition metals within the grains.

II. EXPERIMENTAL PROCEDURES AND SAMPLE PREPARATION

In order to assess the transition metal content of modern photovoltaic-grade mc-Si and compare the metal content of the materials grown using different technologies, instrumental NAA studies were performed on three types of samples, Astropower silicon-film multicrystalline sheet material,[16–18] Baysix cast material,[19] and edge-defined film-fed growth (EFG) ribbon-grown mc-Si.[20,21] Besides the determination of the average metal concentration in each of these three types of material, we compared samples of the same material cleaved from the areas with relatively high and relatively low minority carrier diffusion length.

Since EFG wafers have large (typically 10–15 mm or greater) grains, samples from good and bad grains could be easily cleaved using diffusion length maps. In contrast, Baysix and Astropower samples had grain size in the millimeter range, and cleaving sufficiently large samples, with higher than average or lower than average minority carrier diffusion length, was not possible. Therefore, we compared pieces of wafers with relatively high and relatively low average minority carrier diffusion lengths.

EFG wafers were mapped with the surface photovoltage (SPV) technique using a CMS-IIIA machine. The obtained minority carrier diffusion maps were used to cleave the wafers into samples with average (30–60 μm), lower than average (<20 μm), and higher than average (>80 μm) diffusion length. Baysix samples were cleaved from wafers from the bottom of the ingot (relatively low diffusion length, $L_D = 25$ to 50 μm, according to laser beam-induced current mapping performed at Fraunhofer ISE) and from the middle of the ingot (relatively high diffusion length, $L_D = 40$ to 200 μm). Astropower samples were cleaved from two wafers, which were fully processed solar cells with stripped off front and back contacts. One of the two cells had better electrical properties than the other one, with the average carrier lifetime approximately 50% better in the cell with better electrical properties. Our SPV measurements indicated that wafer A, with better electrical properties, had a minority carrier diffusion length of 7.5 ± 0.7 μm at the center of the wafer and 8.8 ± 1.2 μm at the edge, whereas wafer B, with worse electrical parameters, had the diffusion length of 4.4 ± 1.5 μm at the center of the wafer and 5.0 ± 1.5 μm at the edge.

All samples were cleaved to avoid contamination which may be introduced by a mechanical saw. The samples for analyses were weighed, chemically etched, wrapped in clean aluminum foil, irradiated at a nuclear reactor, unwrapped,

TABLE I. Average metal concentration found by neutron activation analysis of three types of multicrystalline silicon material: Astropower (sheet technology), BaySix (cast), and EFG (ribbon growth). DL stands for "detection limit."

Element	Astropower (cm^{-3})	BaySix (cm^{-3})	EFG (cm^{-3})
Fe	1.50×10^{16}	4.00×10^{14}	6.00×10^{14}
Ni	1.80×10^{15}	*less than DL* (3×10^{14})	*less than DL* (1.1×10^{14})
Co	9.70×10^{13}	2.10×10^{13}	1.70×10^{12}
Cu	*less than DL* (7.8×10^{12})	$<2.4\times10^{14}$	$<1.3\times10^{14}$
Cr	1.80×10^{15}	1.00×10^{13}	1.70×10^{12}
Hf	*less than DL* (1.8×10^{12})	7.80×10^{12}	*less than DL* (6.8×10^{11})
Mo	4.60×10^{13}	1.50×10^{13}	6.40×10^{12}
W	2.00×10^{13}	*less than DL* (2.2×10^{11})	*less than DL* (8×10^{10})
Au	4.80×10^{11}	6.50×10^{10}	2.00×10^{10}
As	4.70×10^{13}	3.40×10^{12}	*less than DL* (9.3×10^{10})
Sb	2.40×10^{14}	1.70×10^{12}	1.20×10^{11}
Ga	2.50×10^{13}	*less than DL*	9.00×10^{12}

etched again, and counted at an on-site low background facility or at an off-site underground ultralow background facility at Oroville Dam. Additionally, blank CZ samples were included in each set to control levels of contamination introduced during chemical cleaning and irradiation. Since no transition metals were found in the blank samples, it was concluded that all impurities detected in mc-Si were indeed located within the samples. Details of the equipment and procedures used in NAA analyses can be found in Ref. 22. A typical weight of the samples was 1 to 2 g. Irradiation was performed at the 10 MW University of Missouri Research Reactor and at 2 MW McClellan Nuclear Radiation Center. The total neutron flux was $7.42\times10^{12}\ s^{-1}\,cm^{-2}$ (which consisted of a thermal (typically corresponding to the energies of 0.0253 eV) flux of $6.8\times10^{12}\ s^{-1}\,cm^{-2}$ and an epithermal (fast neutrons with the energies above 1 eV) flux of $5.8\times10^{11}\ s^{-1}\,cm^{-2}$), irradiation time was 36 min in all measurements except for the data presented in Table II, where the neutron flux was $2.67\times10^{13}\ cm^{-3}$ ($2.5\times10^{13}\ s^{-1}\,cm^{-2}$ thermal and $1.4\times10^{12}\ s^{-1}\,cm^{-2}$ epithermal) and the irradiation time was 16 h. The thermal and epithermal ("resonant") flux was determined from counting metal foils with known cross sections for neutrons irradiated together with the samples. Although the neutron irradiation time and flux were higher in the latter case, the impurity detection limits were lower as counting could not commence within a short time after irradiation because of the excessively high radioactivity of the aluminum container used during that irradiation. Each sample was counted at least twice, and the obtained results were cross checked for consistency.

TABLE II. Metal concentration in the areas of EFG samples with higher than average (good) and lower than average (bad) minority carrier diffusion lengths. Due to different irradiation and counting conditions, the detection limits of this measurement run were lower than of the runs presented in Tables I, III, and IV. Therefore, iron and some other metals were below the detection limits.

Element	Good areas (cm^{-3})	Bad areas (cm^{-3})
Cr	2.97×10^{12}	5.94×10^{11}
Mo	7.09×10^{13}	6.00×10^{13}
Sb	8.20×10^{10}	9.00×10^{10}
Au	5.00×10^{11}	3.00×10^{12}

III. NEUTRON ACTIVATION ANALYSIS EXPERIMENTAL RESULTS AND DISCUSSION

The NAA results are presented in the Tables I–IV. Table I is a comparison of the average metal content of the three types of material analyzed in this study. Tables II–IV are comparisons of the metal concentrations in good and bad areas of EFG wafers (Table II), samples cleaved from Baysix (Table III), and Astropower (Table IV) wafers with good and poor electrical properties. The main metal impurities found in the samples were Fe, Ni, Co, Cr, and Mo (Table I). It should be noted that the detection limits of NAA depend on several factors including: the weight of the sample, the natural abundance of the isotope(s) which can be detected after neutron irradiation, half-lifetimes of these isotopes, neutron flux during the irradiation, duration of the irradiation, time elapsed between neutron irradiation and beginning of counting, background radiation at the counting facility, and the

TABLE III. Metal concentration in BaySix wafers with relatively high (middle of the ingot) and relatively low (bottom of the ingot) minority carrier diffusion length. DL stands for detection limit.

Element	Sample A (middle of the ingot, better cell performance) (cm^{-3})	Sample B (bottom of the ingot, lower cell performance) (cm^{-3})
Ag	3×10^{12}	*less than DL* (5×10^{11})
Cr	1.9×10^{13}	*less than DL* (3×10^{12})
Fe	4.7×10^{14}	*less than DL* (4.5×10^{14})
Ni	*less than DL* (3×10^{14})	*less than DL* (2.3×10^{14})
Co	8×10^{12}	2.80×10^{13}
As	3.80×10^{12}	2.90×10^{12}
Sb	3.70×10^{11}	3.20×10^{12}
W	*less than DL* (1×10^{11})	*less than DL* (3.6×10^{11})
Au	1.50×10^{10}	1.20×10^{11}
Zr	3.3×10^{14}	3.5×10^{14}
Hf	1.40×10^{13}	*less than DL* (1.1×10^{12})
Cu	$<1.6\times10^{14}$	$<3.2\times10^{14}$
Se	2×10^{13}	4×10^{12}
Mo	1.50×10^{13}	*less than DL* (5.4×10^{13})

TABLE IV. Metal concentration in Astropower wafers with relatively high ("wafer A") and relatively low ("wafer B") minority carrier diffusion length areas. DL stands for detection limit.

Element	Wafer A (better cell performace) (cm^{-3})	Wafer B (lower cell performance) (cm^{-3})
Cr	3×10^{15}	5×10^{13}
Fe	1.6×10^{16}	8.7×10^{15}
Ni	2.8×10^{15}	*less than DL* (5×10^{15})
Co	1.3×10^{14}	6.1×10^{13}
Cu	*less than DL* (5×10^{12})	*less than DL* (1×10^{13})
Ga	2×10^{12}	*less than DL* (3×10^{12})
As	9×10^{13}	3.5×10^{12}
Zr	*less than DL* (1.5×10^{15})	*less than DL* (4×10^{15})
Hf	*less than DL* (1.1×10^{12})	*less than DL* (3×10^{12})
Mo	6×10^{13}	3×10^{13}
Sb	2×10^{13}	5×10^{14}
W	2×10^{13}	2×10^{13}
Au	3.5×10^{11}	4×10^{11}

counting time. Hence, the detection limits for the same metal varied from sample to sample, and were substantially different for different metals in the same sample.

The main conclusion which can be drawn from Table I is that all detected metals were present in surprisingly high concentrations, consistent with the recent report of Macdonald *et al.*[6] The primary contaminants in all three materials were Fe, Ni, and Cr, which may be an indication of contamination with stainless steel. Copper was also detected, but its concentration could not be determined accurately because of the short lifetime (12.7 h) of the corresponding radioactive isotope. The data presented in Table I for copper are upper limits. Although Table I lists the metal content of three different materials side by side, one should be cautious and refrain from generalizing the differences in metal content in different mc-Si materials for two reasons. First, Astropower samples used in this study were cleaved from fully processed solar cells after the removal of the top and bottom contact layers, whereas Baysix and EFG were as-grown wafers which did not get processed. Second, it is known that transients in impurity distribution are common to all techniques of crystal growth from the melt. As a growth run proceeds and melt volume decreases, the concentration of metals segregated in the melt gets higher, and an increasingly large quantity of metals gets incorporated in the crystal toward the tail part of the ingot. In mc-Si fabrication, the nature of transient effects may be quite complicated as they are affected, e.g., by feedstock replenishment, thermal gradients, and growth run interruptions. Hence, the metal content of each material may vary in a fairly wide range, which might affect the ratio between concentrations of metals found in different types of materials.

An analysis of samples cleaved from the areas with high and low minority carrier diffusion lengths (Tables II–IV) revealed that the difference in metal concentration in good and bad areas is small. Only gold was consistently found in the bad areas in 1.5 to 5 times higher concentrations than in the good areas of all three materials. The rest of the metals detected by NAA showed either no trend at all, or, in some cases, metals were even found in slightly higher concentration in the good areas.

Remarkably, the total transition metal concentrations observed in all three mc-Si materials were much higher than necessary to explain the minority carrier lifetime degradation in these materials. For example, only approximately 2×10^{13} cm^{-3} of FeB pairs, or 2×10^{12} cm^{-3} of interstitial iron is sufficient to reduce the diffusion length to 50 μm; 2×10^{15} cm^{-3} of FeB or 2×10^{14} cm^{-3} of Fe_i would reduce the diffusion length to 5 μm.[3] In each of the three types of the mc-Si materials, the average concentration of iron alone was at least ten times higher than it would be sufficient, if all iron were in the interstitial state, to account for the carrier recombination responsible for the measured minority carrier diffusion length. The other transition metals found in the samples, particularly Cr and Mo, have a recombination activity comparable with that of iron[23,24] and can also substantially contribute to the minority carrier diffusion length degradation. Therefore, either transition metals are present in relatively recombination inactive chemical/structural state, or they are extremely inhomogeneously distributed in the wafer, or both. In either case, only a small fraction (anywhere between 1% and 10%) of the total metal concentration controls the minority carrier diffusion length, along with other structural defects in the silicon lattice which may be recombination active. A small variation in the chemical/structural state of metals which leads to a change in their recombination properties may account for the difference between good and bad grains in solar cells, regardless of the total metal content of these grains.

Thus, two conclusions can be made from the results of our NAA analysis. First, it is extremely likely that transition metals substantially contribute to, if not determine, the minority carrier diffusion length degradation in solar cells. In fact, it is surprising that material with such a high metal content (over 4×10^{14} cm^{-3} of iron and over 10^{12} cm^{-3} of Cr and Mo) may perform so well when processed into solar cells. The relatively low recombination activity of these metals (as compared to that of interstitial/substitutional metals) can be tentatively explained by assuming that the metals are present chiefly in the form of precipitates or agglomerates with other structural defects of the crystal lattice, and are possibly inhomogeneously distributed in the wafers. Although metal precipitates are known to be recombination active, it is possible that, at least in some chemical/structural states, the recombination activity of a precipitate per metal atom is much lower than the recombination activity of homogeneously distributed in the bulk interstitital/substitutional metal atoms.

The electrical and recombination properties of metal precipitates, most notably Ni and Cu, were studied recently.[25–28] An important finding reported in Refs. 25–28, common for Ni and Cu precipitates, is that such precipitates form band-like defect states in the silicon band gap. These precipitates are very efficient for carrier recombination and yet cannot be easily detected by electrical techniques such as deep level transient spectroscopy (DLTS) unless the precipitates are present in very high concentrations. This is because the DLTS peaks associated with these precipitates are unusually

wide, which makes their apparent amplitude much lower than the actual density of defect-related states. Hence, metal clusters may form recombination active defect bands which affect lifetime, but avoid detection by DLTS.

IV. MICROPROBE X-RAY FLUORESCENCE ANALYSIS OF THE SAMPLES

To confirm that metals indeed form clusters and are inhomogeneously distributed in the mc-Si samples, we applied advanced synchrotron-radiation based x-ray techniques to analyze the Astropower material. The measurements were performed at Beamline 10.3.1 of the Advanced Light Source (synchrotron facility) at the Lawrence Berkeley National Laboratory. This beamline is used for high-resolution μ-XRF mapping studies. An intense x-ray beam from the synchrotron, with approximately 10^{10} photons/s, is incident on the sample, focused to an optimal spot size of $(1-2)\times(1.5-3)$ μm^2 by a pair of elliptically bent multilayer mirrors in a Kirkpatrick–Baez configuration. Horizontal and vertical slits determine the amount of beam incident on the mirrors and make it possible to independently vary the vertical and horizontal dimensions of the spot size from approximately 1 to 6 μm. The emanating x-ray fluorescence (XRF) is detected by a Si:Li detector. The sampling depth of this technique is determined by the escape depth of the fluorescence x-rays of interest from the silicon matrix, typically between 10 and 100 μm depending on the element. The sensitivity of the XRF tool depends on the accumulation time at each point, and is typically sufficient to detect a single iron precipitate with a radius of 30–45 nm, or dissolved iron in concentration of about 10^{14} per cm^2 on the sample surface. In addition to analyzing the distribution of metals, their recombination activity can be characterized *in situ* and simultaneously with the μ-XRF scan by the x-ray beam-induced current technique [(XBIC) Ref. 29]. Further details of this experimental system and some examples of its applications can be found elsewhere.[30,31]

A piece of as-grown Astropower SiliconFilm™ sheet material was aluminum gettered at 800 °C for 4 h in our lab, so that only the most gettering-resistant metal precipitates remained in the material. To determine the precise location of the gettering-resistant metal precipitates, an XBIC scan covering several square millimeters was performed. Within this XBIC map, regions of interest were identified by their lower than average diffusion length, appearing as dark features in the XBIC maps. Subsequently, μ-XRF/XBIC line or area scans were performed in these regions of interest to establish the presence of transition metals.

Transition metal precipitates were found at and near structural defects, such as grain boundaries. Illustrated in Fig. 1(a) is a two-dimensional XBIC scan of a grain boundary. Noticeable is a circular outgrowth of lower collected current, indicative of a recombination active precipitate, demarcated by the arrow in the XBIC map in Fig. 1. To confirm the presence of transition metals, a μ -XRF line scan [Fig. 1(b)] was performed along the vertical dotted line shown in the XBIC image [Fig. 1(a)]. One can see that iron was found at the grain boundary, corresponding with the largest decrease in XBIC signal.

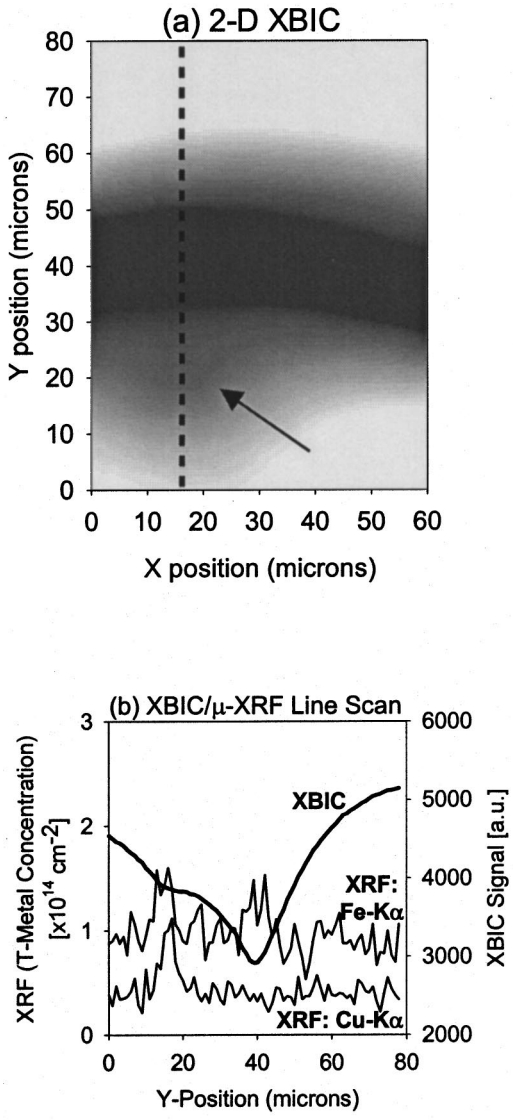

FIG. 1. XBIC map (a) and μ-XRF profile of metal distribution across a grain boundary (b). The μ-XRF profile was taken along the dashed line shown on the XBIC map on the left-hand side. The grain boundary corresponds to the dark contrast going from the left- to right-hand side through the middle of the XBIC map. Note a metal cluster adjacent to the boundary, indicated by an arrow in (a). XRF profile in (b) shows that this metal cluster contains iron and copper, whereas only iron was found at the grain boundary.

Of special interest in Fig. 1 is the complex consisting of copper and iron, indicated by the arrow in Fig. 1(a) and located approximately 25 μm away from the grain boundary in question. This complex, containing roughly an equivalent amount of iron and substantially more copper than the grain boundary, is less recombination active, evidenced by the smaller decrease in XBIC signal. One explanation is simply that the precipitate lies deep below the surface within the bulk, and all of the electron–hole pairs generated between the precipitate and the surface are collected, thereby yielding a higher XBIC signal than if the precipitate were sitting near the surface. An alternate explanation could be that the copper, coprecipitated with iron, could passivate the electrically active iron precipitate. Such passivation effects of Cu result-

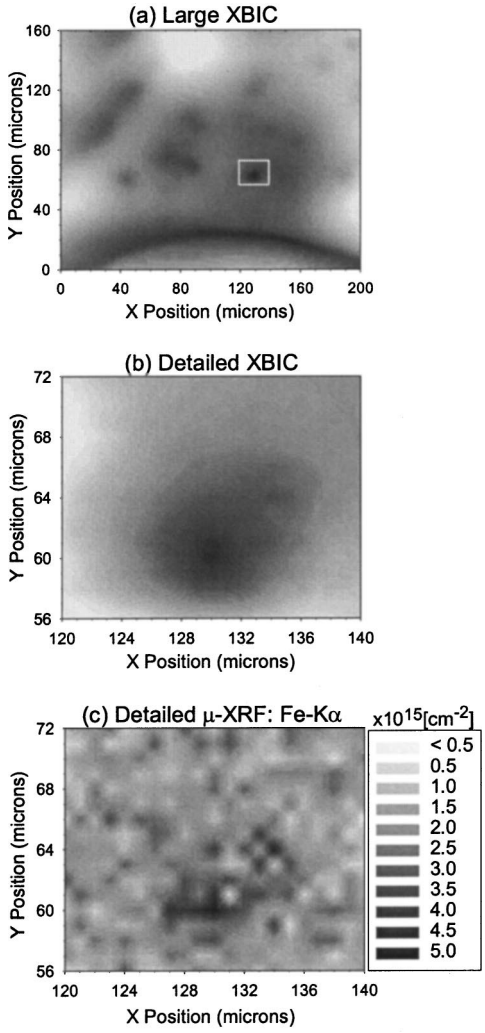

FIG. 2. XBIC [(a) and (b)] and μ-XRF Fe (c) maps of an intragranular metal cluster in Astropower material. The μ-XRF image in (c) corresponds to the area demarcated by a rectangle in the XBIC plot (a) and shown on a more detailed scale in (b).

ing in increased carrier diffusion length were recently observed.[32]

The observation of iron at the grain boundary is not surprising as grain boundaries were long thought to serve as precipitation (gettering) sites for transition metals such as iron.[31,33–35] In addition, regions of enhanced minority carrier diffusion length (denuded zones) in the immediate vicinity of grain boundaries were identified with XBIC, suggesting a lower concentration of recombination active defects in these regions. This can be a consequence of gettering of iron by the grain boundary from the adjacent areas (see, e.g., Ref. 36), further exacerbated by a lower density of stacking faults/microdefects detectable by selective etching in the vicinity of grain boundaries in Astropower material.[37]

Metal clusters were also found inside the grains. In Figs. 2(a) and 2(b), an XBIC scan is shown. Many dark spots appear within the grain, indicative of highly localized intragranular recombination centers. One of these spots, demarcated by a rectangle in the XBIC scan [Fig. 2(a)], was scanned with μ-XRF [Fig. 2(c)]. Iron appears to be the most abundant contaminant present at this localized area of low diffusion length. Such intragranular precipitates were common in this material, as many others were observed. The concentration of iron at intragranular locations, suggestive of intragranular gettering sites, may in fact be largely responsible for the increased diffusion length within the grains. Provided that iron can diffuse to these gettering sites during heat treatments, and that the minority carrier capture cross sections of these precipitates are sufficiently smaller than the distance between them, they may actually serve to improve the diffusion length within the grains by concentrating iron at select locations, consequently decreasing the concentrations of interstitial iron and the iron–boron pairs dispersed within the grains. The precondition of this mechanism to be beneficial for the overall diffusion length of a specific grain is that the density of these intragranular gettering sites is not too high, in order to create large intragranular volumes of low carrier recombination.

Baysix and EFG materials also contained metal precipitates, but the number of large precipitates and the average size of these precipitates were smaller; a direct consequence of these materials containing less transition metals.

V. SUMMARY AND CONCLUSIONS

Our NAA results bear important consequences for the understanding of the limitations and problems with gettering and passivation of transition metals in solar cells. It is known that standard gettering techniques are not very efficient in removing metals from solar cells. For example, the Astropower wafers used in this study were processed into solar cells (which includes Astropower proprietary gettering treatment) before metallization was stripped off and the material was analyzed by NAA. And yet, this material contains very high concentrations of transition metals.

There are two possible explanations for the low efficiency of gettering techniques for mc-Si. The first one is that at least some of the metals form gettering-resistant clusters, which cannot be dissolved at the gettering temperatures due to high binding energy of the metals in these compounds. The possibility of this mechanism follows from the data of McHugo *et al.*,[13] who detected clusters with the chemical state of iron similar to iron oxide or iron silicate in a processed solar cell, and observed copper clusters which might have a higher stability than expected for copper silicide.[15,38]

The second possible mechanism of low efficiency of gettering in solar cells is kinetically limited precipitate dissolution. This mechanism was suggested by Plekhanov *et al.*[39] They argued that gettering at temperatures at which the equilibrium metal solubility is much lower than the total metal concentration in the sample would lead to extremely long gettering times necessary to achieve an improvement in the minority carrier diffusion length. Consider the following example. At a temperature of 800 °C, typical for aluminum gettering, the solubility and diffusivity of iron are $S(\mathrm{Fe}) = 3\times10^{12}\ \mathrm{cm}^{-3}$ and $D(\mathrm{Fe}) = 7\times10^{-7}\ \mathrm{cm}^2/\mathrm{s}$, respectively. In a wafer containing $6\times10^{14}\ \mathrm{cm}^{-3}$ of Fe, the solubility of iron limits the iron concentration that can be dissolved at a given time to only 0.5% of the total amount of iron present in the wafer. The average time required for this dissolved iron

to diffuse the average distance to the gettering layer equal to one half of the wafer thickness is about 2 min at 800 °C, after which the next portion or iron can be dissolved. Hence, one can roughly estimate the time required for total dissolution and gettering of all iron as 6–8 h even in the absence of any barriers for dissolution. This estimate is in agreement with more rigorous modeling of Plekhanov *et al.*[39] and with extended high-temperature aluminum gettering experiments by Joshi *et al.*[40]

The observation that there was no significant difference in metal concentration observed in good and bad areas of solar cells suggests that the recombination properties of metals may vary in a wide range depending on their chemical or structural state. Therefore, one does not necessarily have to remove the metals from the cells; it is sufficient to convert them to a less recombination efficient state to minimize their impact on the cell performance. This approach can be called metal passivation through defect engineering. Unfortunately, such engineering is not possible at the present time without additional research efforts aimed at understanding the chemical state of metals in solar cells and defect reactions which can be used to convert metal impurities to the desired state.

In summary, NAA studies have shown that mc-Si materials for solar cell applications contain significant concentrations of transition metal impurities, notably Fe, Ni, Co, Mo, and Cr; Cu was also detected, but its concentration could not be accurately determined. Since the concentration of each of these metals was much higher than the concentration sufficient to limit the minority carrier diffusion length at a level typical for each of these materials, it was concluded that the metals are primarily present in the form of precipitates or agglomerates, probably formed at structural defects in the wafers. The ratio of concetrations of Fe, Ni, and Cr indicates the possiblilty of contamination of wafers with stainless steel. μ-XRF analyses confirmed that metals are indeed inhomogeneously distributed in the wafers; metal clusters were found both at the grain boundaries and the intragranular defects. No substantial differences between the metal content of good and bad grains were found. It was suggested that it is not as much the total metal concentration, but rather the spatial distribution and chemical state of metals that determine their recombination activity in solar cells. The relatively low efficiency of gettering in solar cells was tentatively explained by a combination of kinetic limitations for dissolution of metal clusters at the gettering temperatures (i.e., very long annealing times are required) and strong chemical binding of metals in the agglomerates which slows down their dissolution.

ACKNOWLEDGMENTS

This work was funded by NREL Subcontract No. AAT-2-31605-03 and the AG-Solar project of the government of Northrhein-Westfalia (NRW), funded through the Fraunhofer Institute for Solar Energy Systems (ISE) (Germany). The operations of the Advanced Light Source at Lawrence Berkeley National Laboratory are supported by the Director, Office of Science, Office of Basic Energy Sciences, Materials Sciences Division, of the U.S. Department of Energy under Contract No. DE-AC03-76SF00098.

[1] M. A. Green, K. Emery, D. L. King, S. Igari, and W. Warta, Prog. Photovoltaics **11**, 347 (2003).
[2] A. Rohatgi, J. R. Davis, R. H. Hopkins, and P. G. McMullin, Solid-State Electron. **26**, 1039 (1983).
[3] A. A. Istratov, H. Hieslmair, and E. R. Weber, Appl. Phys. A: Mater. Sci. Process. **70**, 489 (2000).
[4] J. H. Reiss, R. R. King, and K. W. Mitchell, Appl. Phys. Lett. **68**, 3302 (1996).
[5] J. P. Kalejs, B. R. Bathey, J. T. Torenstein, and R. W. Stormont, in *Conference Record of the 23rd IEEE Photovoltaics Specialist's Conference* Louisville, KY (IEEE, New York, 1993), p. 184.
[6] D. Macdonald, A. Cuevas, A. Kinomura, and Y. Nakano, in *Proceedings of the 29th Photovoltaic Specialists Conference* New Orleans, LA (IEEE, New York, 2002), p. 285.
[7] B. L. Sopori, Mater. Sci. Forum **258**, 527 (1997).
[8] B. Sopori, C. Wei, K. Nemire, J. Gee, and S. Ostapenko, in *Defect and Impurity Engineered Semiconductors II*, edited by S. Ashok, J. Chevallier, K. Sumino, B. L. Sopori, and W. Gotz (Mat. Res. Soc., Warrendale, PA, 1998), p. 505.
[9] J. Bailey and E. R. Weber, Phys. Status Solidi A **137**, 515 (1993).
[10] M. Werner, H. J. Möller, and E. Wolf, Mater. Res. Soc. Symp. Proc. **469**, 89 (1997).
[11] S. A. McHugo, J. Bailey, H. Hieslmair, and E. R. Weber, J. Electron. Mater. **25**, 1417 (1994).
[12] S. A. McHugo, A. C. Thompson, I. Perichaud, and S. Martinuzzi, Appl. Phys. Lett. **72**, 3482 (1998).
[13] S. A. McHugo, A. C. Thompson, G. Lamble, C. Flink, and E. R. Weber, Physica B **273**, 371 (1999).
[14] S. A. McHugo, A. C. Thompson, A. Mohammed, G. Lamble, I. Perichaud, S. Martinuzzi, M. Werner, M. Rinio, W. Koch, H. U. Hoefs, and C. Haessler, J. Appl. Phys. **89**, 4282 (2001).
[15] S. A. McHugo, A. Mohammed, A. C. Thompson, B. Lai, and Z. Cai, J. Appl. Phys. **91**, 6396 (2002).
[16] J. S. Culik, I. S. Goncharovsky, J. A. Rand, and M. Barnett, Prog. Photovoltaics **10**, 119 (2002).
[17] R. B. Hall, A. M. Barnett, J. E. Brown, J. C. Checchi, D. H. Ford, C. L. Kendall, W. P. Mulligan, J. A. Rand, and T. R. Ruffins, U.S. Patent No. 5,336,335 (1994).
[18] R. B. Hall, A. M. Barnett, J. C. Checchi, D. H. Ford, C. L. Kendall, and J. A. Rand, U.S. Patent No. 6,207,891 (2001).
[19] C. Hassler, E.-U. Reisner, W. Koch, A. Muller, D. Franke, and T. Rettelbach, Solid State Phenom. **67**, 447 (1999).
[20] R. O. Bell and J. P. Kalejs, J. Mater. Res. **13**, 2732 (1998).
[21] J. P. Kalejs, Sol. Energy Mater. Sol. Cells **72**, 139 (2002).
[22] A. R. Smith, R. J. McDonald, H. Manini, D. L. Hurley, E. B. Norman, M. C. Vella, and R. W. Odom, J. Electrochem. Soc. **143**, 339 (1996).
[23] J. R. Davis, A. Rohatgi, R. H. Hopkins, P. D. Blais, P. Rai-Choudhury, J. R. McCormic, and H. C. Mollenkopf, IEEE Trans. Electron Devices **ED-27**, 677 (1980).
[24] R. H. Hopkins and A. Rohatgi, J. Cryst. Growth **75**, 67 (1985).
[25] A. A. Istratov, H. Hedemann, M. Seibt, O. F. Vyvenko, W. Schröter, T. Heiser, C. Flink, H. Hieslmair, and E. R. Weber, J. Electrochem. Soc. **145**, 3889 (1998).
[26] A. A. Istratov and E. R. Weber, Appl. Phys. A: Mater. Sci. Process. **66**, 123 (1998).
[27] F. Riedel and W. Schröter, Phys. Rev. B **62**, 7150 (2000).
[28] M. Kittler, J. Larz, W. Seifert, M. Seibt, and W. Schröter, Appl. Phys. Lett. **58**, 911 (1991).
[29] O. F. Vyvenko, T. Buonassisi, A. A. Istratov, H. Hieslmair, A. C. Thompson, R. Schindler, and E. R. Weber, J. Appl. Phys. **91**, 3614 (2002).
[30] S. A. McHugo, A. C. Thompson, C. Flink, E. R. Weber, G. Lamble, B. Gunion, A. MacDowell, R. Celestre, H. A. Padmore, and Z. Hussain, J. Cryst. Growth **210**, 395 (2000).
[31] O. F. Vyvenko, T. Buonassisi, A. A. Istratov, E. R. Weber, M. Kittler, and W. Seifert, J. Phys.: Condens. Matter **14**, 13079 (2002).
[32] A. A. Istratov and E. R. Weber, J. Electrochem. Soc. **149**, G21 (2002).
[33] A. Ihlal and G. Nouet, Phys. Status Solidi A **141**, 81 (1994).
[34] A. Ihlal and R. Rizk, J. Phys. D **29**, 3096 (1996).
[35] J. L. Maurice and C. Colliex, Appl. Phys. Lett. **55**, 241 (1989).

[36] M. Kittler, W. Seifert, M. Stemmer, and J. Palm, J. Appl. Phys. **77**, 3725 (1995).
[37] J. Lu, J. Rand, R. Jonczyk, and G. A. Rozgonyi, in *Proceedings of the 12th Workshop on Crystalline silicon Solar Cell Materials and Processes*, edited by B. L. Sopori (NREL, Golden, CO, 2002), p. 275.
[38] S. A. McHugo and C. Flink, Appl. Phys. Lett. **77**, 3598 (2000).
[39] P. S. Plekhanov, R. Gafiteanu, U. M. Gosele, and T. Y. Tan, J. Appl. Phys. **86**, 2453 (1999).
[40] S. M. Joshi, U. M. Gosele, and T. Y. Tan, Sol. Energy Mater. Sol. Cells **70**, 231 (2001).